SEMARAK ILMU PUBLISHING

Journal of Advanced Research in Fluid Mechanics and Thermal Sciences

Journal homepage:
https://semarakilmu.com.my/journals/index.php/fluid_mechanics_thermal_sciences/index
ISSN: 2811-3950

Model Predictive Control for Regulating Fuel Cell Stack Temperature and Air Flow Rate

Muhammad Abdullah[1], Moumen Idres[1,*], Mohd Azan[1]

[1] Department of Mechanical Engineering, International Islamic University Malaysia, Jalan Gombak, 53100, Kuala Lumpur, Malaysia

ARTICLE INFO

Article history:
Received 14 August 2021
Received in revised form 24 January 2022
Accepted 26 January 2022
Available online 24 February 2022

Keywords:
Proton Exchange Membrane Fuel Cell; Laguerre function; Exponential weight function; Constrained MPC

ABSTRACT

Stack temperature and airflow rate are vital control problems for Proton Exchange Membrane fuel cell (PEMFC). Two separate Model Predictive Controllers (MPC) have been employed to regulate these problems. The controllers utilized Laguerre and exponential weight functions to reduce its numerical instability and computational time. The temperature MPC considered delayed and constrained coolant pump voltage as manipulated input and stack temperature as the desired output. While airflow MPC manipulated compressor motor voltage to maintain the desired level of oxygen excess ratio subjected to starvation, surge, and choke constraints. Results showed that both controllers worked well together. The desired temperature and oxygen excess ratio were maintained subjected to all the constraints, even with the presence of external disturbances. This study highlights that MPC manages to handle both control problems without any conflict. Yet, it also proves that MPC can handle a large time delay process.

1. Introduction

With the growth of energy concerns, there is a high demand for green vehicle technology such as Proton Exchange Membrane Fuel Cell (PEMFC). This system converts the chemical energy of hydrogen and oxygen into electricity while producing heat and water as reactant products without any harmful gases. Although PEMFC offers many benefits, several problems need to be improved, namely its airflow rate and stack temperature control issues [1].

Lack of air induction to the system will lead to starvation, damaging the stack and reducing cell life. Yet, if it is too high, the net power produced is insufficient to operate the vehicle [2]. Besides, a lot of heat is generated during the electrochemical reaction process. This scenario will initiate the rise of stack temperature, leading to hydration and thermal stress in the membrane, which again can reduce cell life [3].

Many research papers have reported successful applications in controlling the air flow rate of PEMFC by using various control methods ranging from classical controllers such as PID and Fuzzy logic [4]. Optimal controllers such as Linear Quadratic Regulator and Model Predictive Control [5-7]. Data-

* *Corresponding author.*
E-mail address: midres@iium.edu.my

https://doi.org/10.37934/arfmts.92.2.171181

driven control such as Adaptive controller and Artificial intelligence-based controller [8,9]. Similarly, a lot of research works regarding the development of PEMFC for stack temperature are published. This includes the modelling process and control applications [10-13].

Based on the review, it is noted that each of these control methods has its advantages and disadvantages. Classical controllers are well established, yet it has poor performance when the system is highly nonlinear [1]. The data-driven controller seems promising; however, there is a lack of guaranteed properties in terms of stability and feasibility. Conversely, an optimal controller such as MPC is also well established in theoretical development, yet one of the main issues is the computation burden [7]. Another critical issue is the integration between the two systems. Most of the works have been only focused on each specific control problem and assumed other issues are well controlled or regulated.

In this work, the integration of two separate MPC based controllers is developed to control both air flow rate and temperature rise of PEMFC. The controllers are separated due to their significant dynamics difference. The main reason for proposing MPC is its ability to handle multivariable systems, time-delay systems, and constraints systems [12,14]. All the operational constraints of PEMFC are considered. Both MPC controllers are formulated with Laguerre and exponential weight functions to reduce the computational time and numerical instability as proposed by Wang [15]. With this modification, the computed solution can provide a large horizon effect by using a small number of parameters.

This paper is organized such that Section 2 presents the MPC formulation for both control problems. Section 3 discusses the results and findings. Section 4 concludes the work.

2. Methodology

2.1 PEMFC Stack Temperature Model

In the previous study, the Pukrushpan's [17] mathematical model that is based on a 75 kW Ballard Mark 700 fuel cell is used to control the airflow rate of PEMFC [7,16]. This control-oriented model has been validated and accepted as a benchmark automotive fuel cell model by the control community [5,11,14]. For simplicity, it assumes that the temperature and humidity are well controlled. To include the temperature effect, an extension model developed by Na and Gou [10] was added to the existing model to represent the stack temperature rise. We selected this model due to its compatibility with the airflow model. A detailed mathematical model is given as:

$$\dot{Q}_{stack} = C_t \frac{dT_{st}}{dt} = P_{total} - P_{elec} - \dot{Q}_{cool} - \dot{Q}_{loss} \tag{1}$$

where

$\dot{Q}_{stack}$: Rate of heat absorption by the stack (Js^{-1})
C_t : Thermal capacitance ($\mathrm{J°C}^{-1}$)
T_{st} : Stack temperature (°C)
P_{total} : Power released by chemical equation (W)
P_{elec} : Power consumed by the load (W)
$\dot{Q}_{cool}$: Heat flow rate of cooling system
$\dot{Q}_{loss}$: Heat flow rate through the stack surface

The total energy is expressed by the rate of hydrogen consumption as:

$$P_{total} = \dot{m}_{H_2\_used}\Delta H = \frac{N_{fc}I_{st}}{2F}\Delta H \quad (2)$$

where

ΔH : Hydrogen enthalpy change ($28.5\ \mathrm{kJmols}^{-1}$)
$\dot{m}_{H_2\_used}$: Hydrogen consumption rate
N_{fc} : Number of fuel cell stack (381)
I_{st} : Stack current
F : Faraday constant

The electrical power output is:

$$P_{elec} = V_{st}I_{st} \quad (3)$$

The rate of heat removal by cooling water is:

$$\dot{Q}_{cool} = \dot{m}_{cool\_water}C_p\Delta T_{st} \quad (4)$$

The specific heat coefficient of water C_p is given as 4182 J/kg K, and the allowable temperature rise $\Delta T_{st} = 10\ K$. The water pump flow $\dot{m}_{cool\_water}$ (Kg/sec) is:

$$\dot{m}_{cool\_water} = \frac{k_c}{1+\tau_c s}u_{cl} \quad (5)$$

where τ_c is the time delay constant, 70 sec, k_c is the conversion factor, 0.365, which means that for u_{cl} range of 0 V to 10 V, $\dot{m}_{cool\_water}$ range is 0 to 3.65 (Kg/s) with 70 second delay.

The heat loss by the surface of the stack is:

$$\dot{Q}_{loss} = hA_{st}(T_{st} - T_{amb}) \quad (6)$$

where the stack heat transfer hA_{st} is 17 WK^{-1} and the ambient temperature T_{amb} is 298 K. The thermal capacitance C_t for this problem is 35 (kJK^{-1}). The continuous state space matrix coefficients were formed as:

$$A = \begin{bmatrix} -4.86E-4 & -1.1949 \\ 0 & -0.0143 \end{bmatrix}$$
$$B = \begin{bmatrix} 0.0161 & -2.86E-5 & 4.86E-4 & 0 \\ 0 & 0 & 0 & 0.0052 \end{bmatrix} \quad (7)$$
$$C = [1 \quad 0]$$
$$D = [0 \quad 0 \quad 0 \quad 0]$$

Figure 1 shows the open-loop structure of thermal behaviour. A continuous linear state space temperature model was constructed as:

$$x_{k+1} = Ax_k + B\bar{u}_k$$
$$y_k = Cx_k + D\bar{u}_k \quad (8)$$

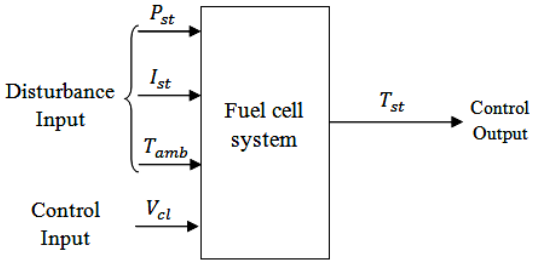

Fig. 1. PEMFC open-loop structure

The states (*x*), output (*y*), and input ($\bar{u}$) are selected as:

$$x = [T_{st}\ \tau_c]^T$$
$$y = T_{st} \quad (9)$$
$$\bar{u} = [u_{cl} \mid P_{st}\ I_{ts}\ T_{amb}] = [u \mid w]$$

Noted that the system input ($\bar{u}$) was partitioned into controlled input (*u*) and disturbance input (*w*).

2.2 MPC Formulation

Since the temperature dynamics is very slow compared to the oxygen excess ratio, we separated it from each other. According to Pukrushpan [17], the ideal operating temperature is 80°C. The control objective is to track the temperature to its ideal level even with the presence of various disturbances. For MPC formulation, the disturbance inputs, *w* were not included and assumed as external disturbances. MATLAB® c2d function was exploited to convert the model in Eq. (8) into discrete form as:

$$x_{k+1} = Ax_k + Bu_k$$
$$y_k = Cx_k + Du_k \quad (10)$$

where (*k*) is the sampling time index. The model in different form is:

$$\Delta x_{k+1} = A\,\Delta x_k + B_u\,\Delta u_k$$
$$y_{k+1} = C\,\Delta x_{k+1} + y_k \quad (11)$$

The coefficient B_u is the first column of the matrix B, $\Delta x_k = x_k - x_{k-1}$, and $\Delta u_k = u_k - u_{k-1}$. The matrix D was absent due to the principle of receding horizon control. It assumes the input u_k cannot affect the output y_k at the same time [15]. Eq. (11) was augmented to embed an integrator as:

$$\overbrace{\begin{bmatrix}\Delta x_{k+1}\\ y_{k+1}\end{bmatrix}}^{\mathbb{x}_{k+1}} = \overbrace{\begin{bmatrix}A & O^T\\ CA & 1\end{bmatrix}}^{\mathbb{A}}\overbrace{\begin{bmatrix}\Delta x_k\\ y_k\end{bmatrix}}^{\mathbb{x}_k} + \overbrace{\begin{bmatrix}B_u\\ CB_u\end{bmatrix}}^{\mathbb{B}}\Delta u_k$$
$$y_k = \overbrace{[O \quad 1]}^{\mathbb{C}}\begin{bmatrix}\Delta x_k\\ y_k\end{bmatrix} \tag{12}$$

where $\mathbb{x}_k = [\Delta x_k\ y_k]^T$ is the new state variables vector, the triplet symbols ($\mathbb{A}$, $\mathbb{B}$, $\mathbb{C}$) is the new augmented parameters, and $O = [0\ 0\ \dots\ 0]^T$ takes the size of the state.

The Laguerre function allows the usage of a large control horizon with a smaller number of parameters based on the identification concept. The Z-transform of the Laguerre function is expressed as:

$$\Gamma_{N,k}(z,a) = \frac{\sqrt{1-a}}{1-az^{-1}}\left(\frac{z^{-1}-a}{1-az^{-1}}\right)^{N-1} \tag{13}$$

where *a* denotes Laguerre pole location and *N* is the number of Laguerre functions. Eq. (13) in a vector form is $L_k = [l_{1,k}\ l_{2,k}\ \dots\ l_{N,k}]$. This function modifies the control input into:

$$\Delta u_{k+i} = \sum_{n=1}^{N} c_{n_k} l_{n_i} = L_i^T \eta \tag{14}$$

with *i* as the future sampling instant, L_i as the vector of Laguerre functions and vector η comprises *N* Laguerre coefficients $(c_1, c_2, \dots, c_N)$ in functions of *k*. This will substitute the usage of control horizon N_C in traditional MPC with parameters *a* and *N*. To ensure the convergence of the functions; we selected the pole within $0 \le a \le 1$. Selecting $a = 0$ and $N = N_C$ will recover the traditional MPC. The prediction of future augmented states is:

$$\mathbb{x}_{k+m|k} = \mathbb{A}^m \mathbb{x}_k + \sum_{i=0}^{m-1} \mathbb{A}^{m+i-1}\mathbb{B}\ L_i^T\ \eta \tag{15}$$

where $\mathbb{x}_{k+m|k}$ represents prediction of the states at sampling instant *m* at *k* horizon window. The cost function of MPC was formulated based on the DLQR principle to gain a similar analysis, tuning and design as shown below:

$$J = \sum_{m=1}^{Np} \mathbb{x}_{k+m|k}^T\ Q\ \mathbb{x}_{k+m|k} + \eta^T R\ \eta \tag{16}$$

with $Q = \mathbb{C}^T\mathbb{C}$, R is the input weight diagonal matrix $(N \times N)$, $\mathbb{x}_{k+m|k} = [\Delta\mathbb{x}_{k+m|k}\ (y_{k+m|k} - r_{s,k})]^T$, and $r_{s,k}$ is the desired output at time instant *k*. The inclusion of desired output in the augmented states will not change the prediction equations since it is always constant. Substituting Eq. (15) to Eq. (16), we obtained:

$$J = 2\eta^T\ \Psi\ \mathbb{x}_k + \eta^T \Omega\ \eta + \sum_{m=1}^{N_p} \mathbb{x}_k^T (\mathbb{A}^T)^m\ Q\ \mathbb{A}^m\ \mathbb{x}_k \tag{17}$$

where:

$$\Psi = \sum_{m=1}^{Np} \Phi_m\ Q\ \mathbb{A}^m$$
$$\Omega = \sum_{m=1}^{Np} \Phi_m\ Q\ \Phi_m^T + R \tag{18}$$
$$\Phi_m = \sum_{i=0}^{m-1} \mathbb{A}^{m+i-1}\ \mathbb{B}\ L_i^T$$

In traditional MPC, a large selection of N_p will result in an ill-conditioned numerical problem. The exponential weights function overcomes this by setting more emphasis on the current time and less emphasis on future time in the optimization process. The exponential weight factor α was inserted in the cost function Eq. (17). This leads to a simple modification of matrices $\mathbb{A}$,$\mathbb{B}$, Q and R in the previous formulation as:

$$\begin{aligned}\mathbb{A} &= \alpha^{-1}\mathbb{A}\\ \mathbb{B} &= \alpha^{-1}\mathbb{B}\\ Q &= \alpha^{-2}Q + (1-\alpha^{-2})P_{\infty}\\ R &= \alpha^{-2}R\end{aligned} \tag{19}$$

where P_{∞} is the solution of the algebraic Riccati equation. The value of α needs to be slightly larger than 1 to ensure closed-loop stability [15]. If α equal to 1, the traditional MPC is recovered. Finally, the cost function was solved to find the optimum solution for η, which satisfy the set point $R_s = 80°\text{C}$ as:

$$\Delta u_k = L_0^T(-\Omega^{-1}\,\Psi\,\mathbb{x}_k) \tag{20}$$

Here, the receding horizon principle is used to find the input at the current sampling time, *k* subjected to the input constraints:

$$0\,V \;\le\; u_{cl} \;\le\; 10\,V \tag{21}$$

2.3 MPC Formulation for Air Flow Control

For air flow rate, the performance variable is the oxygen excess ratio (λ_{O_2}). It is defined as the ratio between supplied oxygen to stoichiometric oxygen. Starvation occurs when oxygen provided is less than the stoichiometric value ($\lambda_{O_2} = 1$), which is the required value for complete combustion of hydrogen. Operating above this value prevents starvation, but the net power delivered is not optimum if it is too high. For this specific fuel cell, the maximum efficiency point (maximum net power) is approximately corresponding to $\lambda_{O_2} = 2$ [17]. This simplifies the controller design to track the desired set point.

Since PEMFC uses a compressor to control the airflow rate, phenomena such as surge and choke may occur [14,16]. Choke occurs at maximum flow rate during step-up in compressor command, while choking triggers during step down at low mass flow rates. Both events can lead to deficiency and devastation of the compressor. It is always desirable to protect the compressor against those conditions. Thus, a constrained MPC was employed subjected to the output constraints as bellow [14]:

$$\begin{aligned}&-0.0506\delta W_{cp} + \delta p_{sm} \le 0.4\\ &0.0203\delta W_{cp} - \delta p_{sm} \le 0.85\\ &1.9 \;\le\; \lambda_{O_2} \;\le\; 2.1\end{aligned} \tag{22}$$

The coefficient W_{cp} is the compressor flow rate and p_{sm} is the supply manifold pressure. A detailed MPC formulation and construction for airflow control is presented in the studies by Abdullah and Idres [7,16].

3. Results

Figure 2 shows the open-loop fuel cell performance for the thermal behaviour where the input disturbance (Figure 2(a)), input motor (Figure 2(b)) and input coolant (Figure 2(c)) are randomly generated. The temperature settling time was larger than the airflow problem (refer to the studies by Abdullah and Idres [7,16]) due to the significant coolant pump delay of 70 *s*. The temperature took about 250 *s* to reach a steady-state, while airflow needs only 0.5 *s* to settle down [7,16]. Since the temperature was uncontrolled, it reached a high, unrealistic value of 130°C. The disparity in length scale necessitates a scaling of the sampling time. The temperature system sampling time was set to 5 s. Table 1 lists the control parameters that were used for this case.

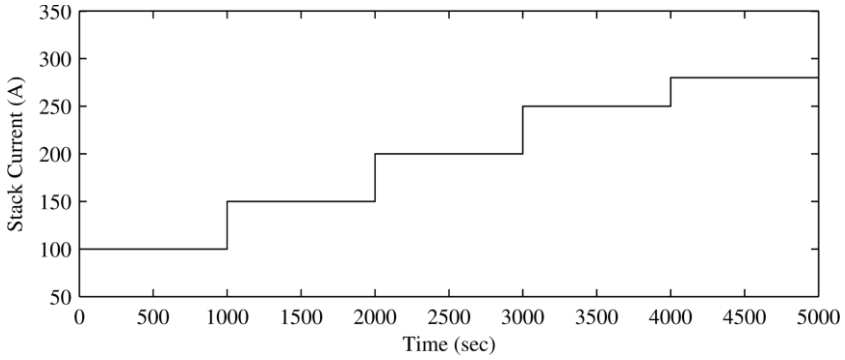

(a)

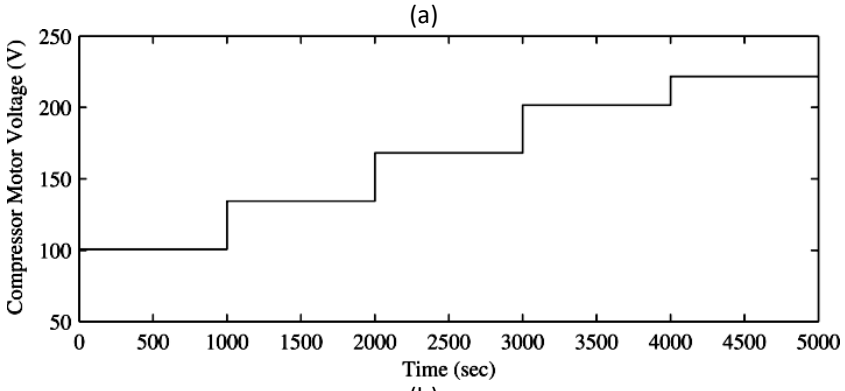

(b)

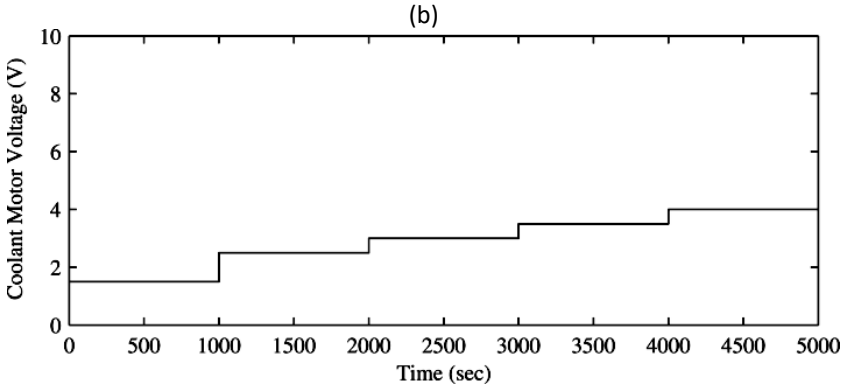

(c)

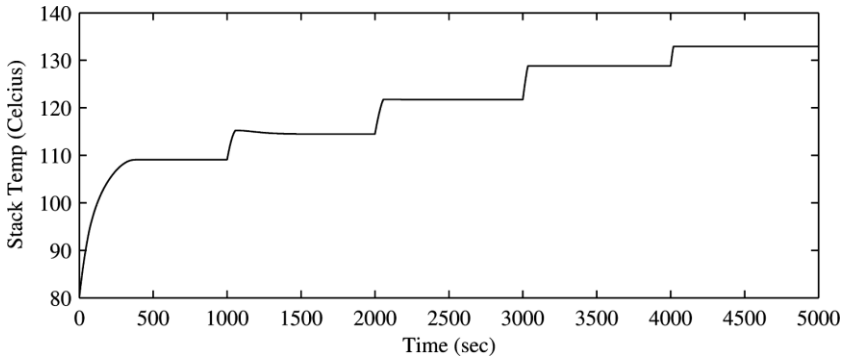

(d)

Fig. 2. Uncontrolled fuel cell temperature behaviour; (a) disturbance input stack current, (b) Input compressor motor voltage, (c) input coolant motor voltage, and (d) output stack temperature

Table 1
MPC parameters for temperature controller

Parameter	Value
N_P	100
N	20
a	0.9
α	1.2
T_S	5 s
R	1

Figure 3 shows the performance of constrained MPC for temperature control. For this case, the input disturbance stack current (Figure 3(a)) is randomly generated, while both input motor voltage (Figure 3(b)) and input coolant voltage (Figure 3(c)) are controlled. The initial temperature was set to 25°C and the setpoint was 80°C (refer to Figure 3(d)). When the input was not constrained, the temperature had a minimum overshoot during the transient period. However, a large coolant motor voltage was needed to obtain this behaviour since the system considered has a large input delay. If this event occurred frequently, it could cause physical damage to the coolant motor due to high over actuation demand. To overcome this issue, the controlled input was constrained to 10 V. As a tradeoff, the temperature produces a higher overshoot during the transient period compared to the unconstrained case, yet within an acceptable range with ±10 degree Celsius.

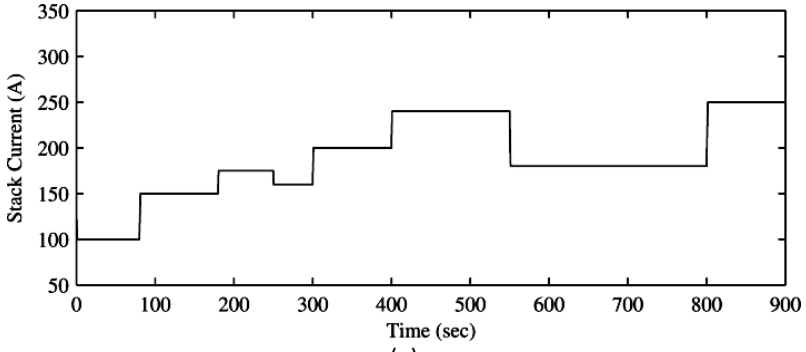

(a)

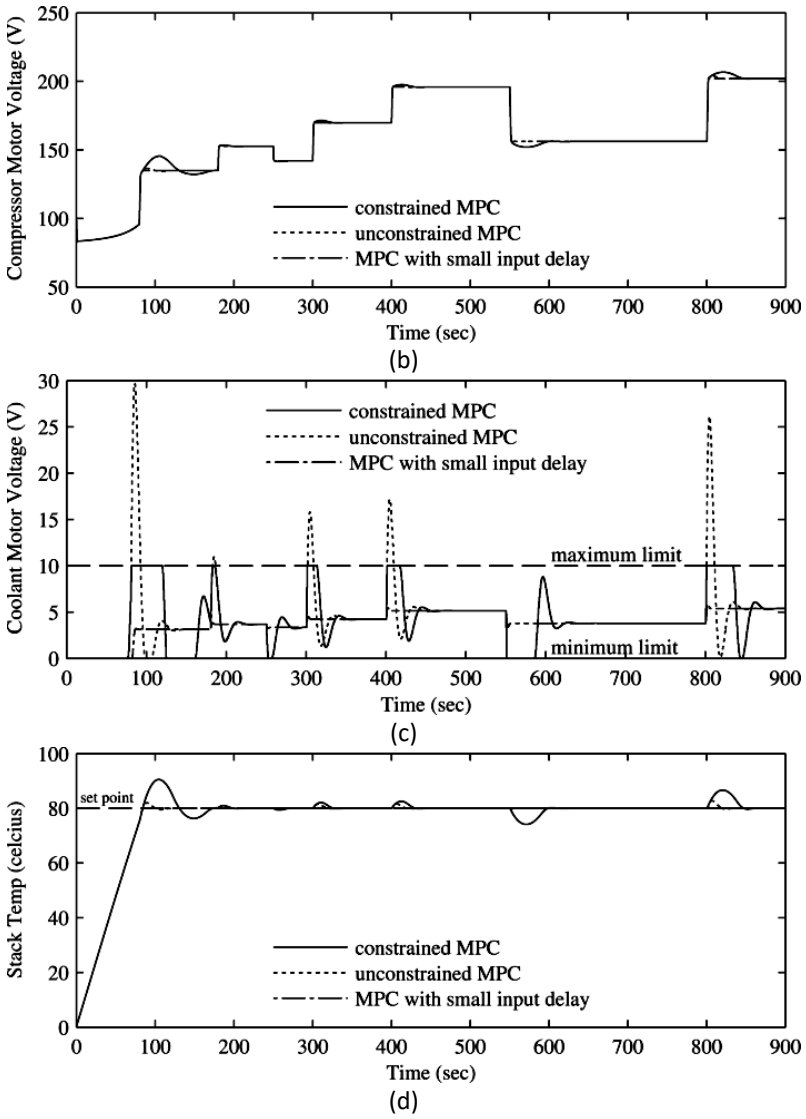

Fig. 3. Controlled fuel cell temperature behaviour; (a) disturbance input stack current, (b) input compressor motor voltage, (c) input coolant motor voltage, and (d) Output stack temperature

Figure 4 presents the controlled airflow performance with constrained outputs in the range of ± 0.1 for the oxygen excess ratio (Figure 4(a)). This behaviour indicated that the airflow controller worked well with the temperature controller. The level of oxygen excess ratio was maintained at the optimum value of 2 without violating the maximum and minimum limits. As for the compressor behaviour (Figure 4(b)), the compressor map respects the surge and choke limit lines. Hence it can be observed that all the constraints on oxygen excess ratio, surge, and choke were satisfied.

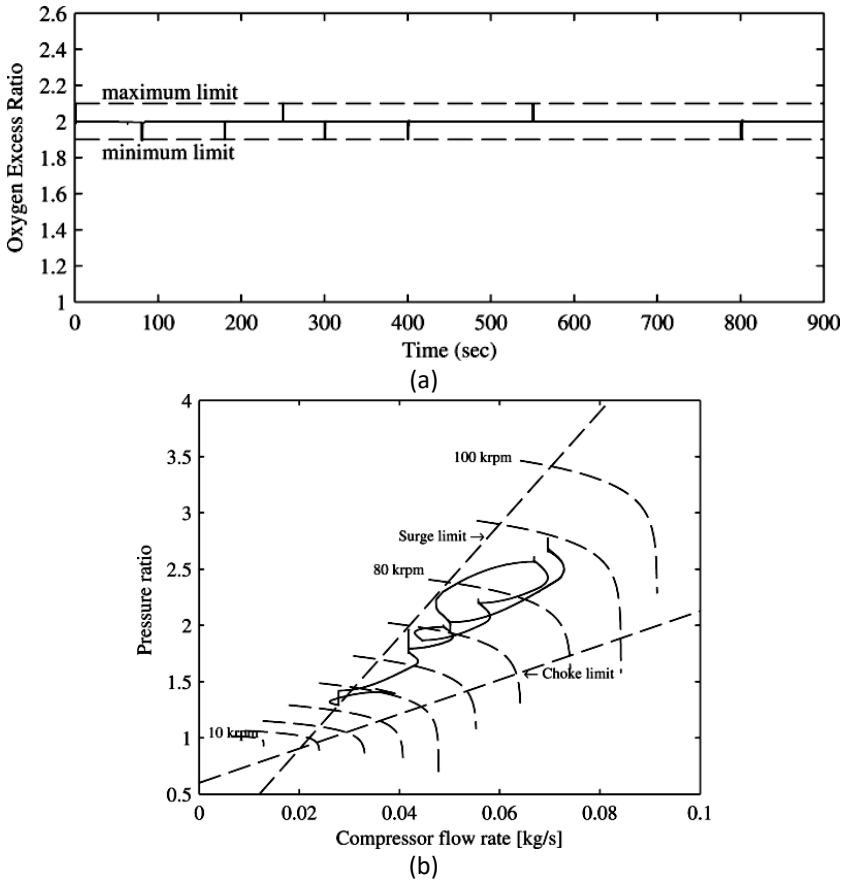

Fig. 4. Constrained PEMFC airflow behaviour; (a) output oxygen excess ratio, and (b) compressor map

4. Conclusions

A linear MPC was developed with Laguerre and exponential weigh functions to track the stack temperature and airflow rate of PEMFC. Both controllers were separated due to their large difference in time scale. Coolant pump delay was considered in the design. Results confirmed that the controller was able to maintain the desired temperature level for multiple-step input current disturbance with an overshoot in the output response due to the coolant pump delay. It is proved that the airflow controller works well with the temperature controller. The level of oxygen excess ratio was maintained at optimum value, and the constraints on oxygen excess ratio, surge, and choke were satisfied. For future work, a modification of MPC to improve the handling of systems with time delay is highly recommendable. The result also needs to be validated via some experimental work.

References

[1] Daud, W. R. W., R. E. Rosli, E. H. Majlan, S. A. A. Hamid, R. Mohamed, and T. Husaini. "PEM fuel cell system control: A review." *Renewable Energy* 113 (2017): 620-638. https://doi.org/10.1016/j.renene.2017.06.027

[2] Hou, Junbo, Min Yang, Changchun Ke, and Junliang Zhang. "Control logics and strategies for air supply in PEM fuel cell engines." *Applied Energy* 269 (2020): 115059. https://doi.org/10.1016/j.apenergy.2020.115059

[3] Zhang, Bo, Fei Lin, Caizhi Zhang, Ruiyue Liao, and Ya-Xiong Wang. "Design and implementation of model predictive control for an open-cathode fuel cell thermal management system." *Renewable Energy* 154 (2020): 1014-1024. https://doi.org/10.1016/j.renene.2020.03.073

[4] AbouOmar, Mahmoud S., Hua-Jun Zhang, and Yi-Xin Su. "Fractional order fuzzy PID control of automotive PEM fuel cell air feed system using neural network optimization algorithm." *Energies* 12, no. 8 (2019): 1435. https://doi.org/10.3390/en12081435

[5] Bordons, Carlos, Alicia Arce, and A. J. Del Real. "Constrained predictive control strategies for PEM fuel cells." In *2006 American Control Conference*, pp. 6-pp. IEEE, 2006. https://doi.org/10.1109/ACC.2006.1656595

[6] Ziogou, Chrysovalantou, Spyros Voutetakis, Michael C. Georgiadis, and Simira Papadopoulou. "Model predictive control (MPC) strategies for PEM fuel cell systems-A comparative experimental demonstration." *Chemical Engineering Research and Design* 131 (2018): 656-670. https://doi.org/10.1016/j.cherd.2018.01.024

[7] Abdullah, Muhammad, and Moumen Idres. "Fuel cell starvation control using model predictive technique with Laguerre and exponential weight functions." *Journal of Mechanical Science and Technology* 28, no. 5 (2014): 1995-2002. https://doi.org/10.1007/s12206-014-0348-3

[8] Sun, Li, Jiong Shen, Qingsong Hua, and Kwang Y. Lee. "Data-driven oxygen excess ratio control for proton exchange membrane fuel cell." *Applied Energy* 231 (2018): 866-875. https://doi.org/10.1016/j.apenergy.2018.09.036

[9] Wang, Xuechao, Jinzhou Chen, Shengwei Quan, Ya-Xiong Wang, and Hongwen He. "Hierarchical model predictive control via deep learning vehicle speed predictions for oxygen stoichiometry regulation of fuel cells." *Applied Energy* 276 (2020): 115460. https://doi.org/10.1016/j.apenergy.2020.115460

[10] Na, Woonki, and Bei Gou. "A thermal equivalent circuit for PEM fuel cell temperature control design." In *2008 IEEE International Symposium on Circuits and Systems*, pp. 2825-2828. IEEE, 2008. https://doi.org/10.1109/ISCAS.2008.4542045

[11] Idres, M., and R. Kafafy. "Dynamic thermal model for proton exchange mambrane fuel cell." In *International Conference on Sustainable Mobility*, pp. 1-10. 2010.

[12] Fan, Yang, and Yang Fu. "Model predictive control for multivariate PEMFC stack temperature system." In *2010 Asia-Pacific Power and Energy Engineering Conference*, pp. 1-4. IEEE, 2010. https://doi.org/10.1109/APPEEC.2010.5449236

[13] Jian, Deng, Quan Shuhai, Hu Shenghui, and Yan Jinchao. "Heat Management Research of a PEMFC System." In *2011 Fourth International Symposium on Knowledge Acquisition and Modeling*, pp. 80-82. IEEE, 2011. https://doi.org/10.1109/KAM.2011.29

[14] Vahidi, Ardalan, Anna Stefanopoulou, and Huei Peng. "Model predictive control for starvation prevention in a hybrid fuel cell system." In *Proceedings of the 2004 American Control Conference*, vol. 1, pp. 834-839. IEEE, 2004. https://doi.org/10.23919/ACC.2004.1383709

[15] Wang, Liuping. *Model predictive control system design and implementation using MATLAB®*. Springer Science & Business Media, 2009.

[16] Abdullah, Muhammad, and Moumen Idres. "Constrained model predictive control of proton exchange membrane fuel cell." *Journal of Mechanical Science and Technology* 28, no. 9 (2014): 3855-3862. https://doi.org/10.1007/s12206-014-0849-0

[17] Pukrushpan, Jay T., Anna G. Stefanopoulou, and Huei Peng. "Control of fuel cell breathing." *IEEE Control Systems Magazine* 24, no. 2 (2004): 30-46. https://doi.org/10.1109/MCS.2004.1275430